Showcasing research from Professor Matsukata's laboratory, Department of Applied Chemistry, Waseda University, Tokyo, Japan.

Self-defect-healing of silicalite-1 membrane in alkaline aqueous solution with surfactant

Defects in zeolite membranes were rapidly healed by immersion into alkaline aqueous solution in the presence of surfactant. This novel defect-healing technique will contribute to improvement for productivity of zeolite membrane.

As featured in:
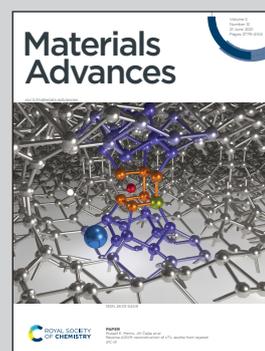
ROYAL SOCIETY OF CHEMISTRY

rsc.li/materials-advances

PAPER

Check for updates

Self-defect-healing of silicalite-1 membrane in alkaline aqueous solution with surfactant†

Motomu Sakai, [iD] *[a] Hayata Hori[b] and Masahiko Matsukata [iD] [c]

Alkaline treatment with surfactant was applied to silicalite-1 membrane for defect healing. By immersion of silicalite-1 membrane into an aqueous solution of sodium hydroxide and cetyltrimethylammonium bromide (CTAB), defects among crystals were sealed, with amorphous silica leached from the membrane itself. During the treatment, the zeolite pores in the membrane were protected by CTAB from excess alkaline etching. As a result, the separation performance of silicalite-1 membrane was successfully improved by this post-treatment without a decrease in permeability due to the collaborative effect of NaOH and CTAB. The separation factor for *n*-hexane/2,3-dimethylbutane mixture increased from 86.5 to 559 after only a 15 min treatment. In addition, the separation performances of other zeolite membranes (Na-*BEA, Na-ZSM-5, and Na-MOR) were also improved by the treatment. This novel defect-healing technique breaks the trade-off line of permeation and separation performance observed with previous post-treatments.

Introduction

Chemical separations require approximately half of all industrial energy and 15% of the total energy consumed in the US.[1] In particular, hydrocarbon separations such as olefin/paraffin and xylene isomer separations for basic chemical production consume large amounts of energy. Membrane separation is fervently anticipated as an energy-efficient, economical, CO_2-free purification process to reduce the energy consumption in chemical production. Membrane separations have the potential for a 10-fold increase in energy efficiency over thermal processes such as distillation, drying, and evaporation.[2]

Zeolite is one of the most promising membrane materials for hydrocarbon separation because of its high thermal, mechanical, and chemical resistance. Zeolites have uniformly sized micropores defined by their crystal structures. The homogeneous distribution of pore size corresponds to superior size-exclusion ability called the molecular sieving property. Therefore, zeolite membranes for hydrocarbon isomer separations have been widely studied.[3–6]

Well-prepared zeolite membranes show high separation performances based on their molecular sieving properties.

However, inter-crystalline defects such as pinholes and cracks in zeolite membranes often degrade the separation performance. Improvement of productivity could be achieved by a simple post-treatment of the membrane, which could reduce membrane costs. For this reason, some post-treatment methods for inter-crystalline defect healing have been reported.[7–11]

The use of silica deposition techniques has been proposed for defect healing in zeolite membranes. Methods used to deposit amorphous silica include the hydrolysis of silicate or the chemical vapor deposition (CVD) method.[7–9] In these methods, amorphous silica is formed in membrane defects and seals them, resulting in the improvement of separation performance. However, the chemicals used in these methods, such as tetraethyl orthosilicate (TEOS) and triethoxyfluorosilane (TEFS), are expensive. Moreover, the equipment for CVD treatment would not be cost-effective.

Defect healing in zeolite membranes by carbon deposition has also been reported. The separation performance of ZSM-5 membrane increased by coking of 1,3,5-triisopropylbenzene immersed in membrane defects.[10] Hong *et al.* reported a method for blocking defects using water-soluble dye molecules.[11] The molecular size of the dye was approximately 1 nm, which was too large to diffuse into the zeolitic pores but was sufficient to selectively block microdefects.

Although the methods described above successfully improved separation performance, there was considerably less permeation due to plugging of the zeolite pores by deposited silica, cokes, and dyes. Then, the challenge remains to develop a simple defect-healing technique that does not result in a decrease in permeability.

[a] *Research Organization for Nano & Life Innovation, Waseda University, 513 Wasedatsurumaki-cho, Shinjuku-ku, Tokyo 162-0041, Japan. E-mail: saka.moto@aoni.waseda.jp*

[b] *Department of Applied Chemistry, Waseda University, 513 Wasedatsurumaki-cho, Shinjuku-ku, Tokyo 162-0041, Japan*

[c] *Advanced Research Institute for Science and Engineering, Waseda University, 513 Wasedatsurumaki-cho, Shinjuku-ku, Tokyo 162-0041, Japan*

† Electronic supplementary information (ESI) available. See DOI: 10.1039/d1ma00364j

Alkaline treatments have been studied for decades as a method to modify zeolite catalysts.[12–16] The mesopores created by traditional alkaline treatments ease the limitation of diffusion in micropores, and then, catalytic properties improve.[12,13] Recently, novel alkaline treatment methods with surfactants or pore-filling agents under relatively mild conditions have been developed.[14–16] Such treatments led to the improvement of not only catalytic properties but also crystallinity and thermal resistance.

We consider that alkaline treatment with surfactant under mild conditions has the potential to heal defects in zeolite membranes. In this study, alkaline treatment with surfactant using sodium hydroxide and cetyltrimethylammonium bromide (CTAB) was carried out for a membrane of silicalite-1, a silicious MFI-type zeolite, to improve separation performance for the first time. The effects of alkaline treatment on crystallinity, defect amounts, and permselectivity were investigated.

Experimental

Membrane preparation

Silicalite-1 membrane was prepared by a secondary growth method according to our previous report.[17] Silicalite-1 seed crystals were loaded on the outer surface of an α-alumina support (o.d. = 10 mm, i.d. = 7 mm, length = 30 mm, average pore size = 150 nm, Noritake Co. Ltd) by a dip-coating technique. Synthesis solution was prepared by mixing distilled water, tetrapropylammonium hydroxide (TPAOH, 1.0 M in H_2O, Sigma-Aldrich), ethanol (>99.5% (GC), Kanto Chemical) and tetraethyl orthosilicate (>99.0% (GC), Sigma-Aldrich).

The molar composition of the synthesis solution was adjusted to $25SiO_2 : 3TPAOH : 1650H_2O : 200EtOH$. Hydrothermal crystallization was conducted at 373 K for 7 days. After crystallization, the membranes were washed with boiling water and dried at 383 K for 12 h. The dried silicalite-1 membrane was calcined at 773 K for 8 h to remove TPA cation occluded in the zeolite framework prior to use.

Alkaline treatment with surfactant

Alkaline treatment of the silicalite-1 membrane was performed with aqueous solution of 0.1 M NaOH (>97.0%, Kanto Chemical) and 0.05 M cetyltrimethylammonium bromide (CTAB, MP Biomedicals). Next, 0.320 g of NaOH and 1.458 g of CTAB were dissolved in 80 g of distilled water in a Teflon beaker. The aqueous solution was pre-heated to 353 K while stirring for 30 min. Silicalite-1 membrane was immersed in the aqueous solution at 353 K, and the solution was stirred for a given period. After that, the silicalite-1 membrane was washed with boiling water to remove the aqueous solution, and then dried at 383 K overnight. The dried silicalite-1 membrane was calcined in a furnace under atmospheric pressure at 673 K for 3 h with a heating rate of 3 K min^{-1}.

Separation tests and characterizations were carried out after calcination. The sequence of separation test, XRD measurement, nano-permporometry, N_2 adsorption, and alkaline treatment was repeated for the same membrane. The accumulated alkaline treatment periods were fixed for 5, 15, 30, 45, and 70 min.

Permeation and separation tests

The permeation and separation tests for the silicalite-1 membrane were carried out in vapor permeation mode. The vaporized equimolar mixture of n-hexane and 2,3-dimethylbutane was fed to the outer surface of the silicalite-1 membrane. The membrane temperature was maintained at 373, 423, 473, and 573 K. The permeable side was swept with Ar gas. Both the feed and permeable sides were maintained at atmospheric pressure.

The permeate was analyzed by gas chromatography (GC-8A, Shimadzu). Flux (J_X) and permeance (P_X) were calculated using the following equations.

$$J_X \text{ (mol m}^{-2}\text{ s}^{-1}) = u_X A^{-1} \tag{1}$$

$$\Pi_X \text{ (mol m}^{-2}\text{ s}^{-1}\text{ Pa}^{-1}) = J_X \Delta P_X^{-1} \tag{2}$$

where u_X denotes the flow rate (mol s^{-1}) of component X, A denotes the membrane area (m^2), and ΔP_X denotes the partial pressure difference of X between the feed and permeable sides (Pa). The separation factor, α, was calculated as the following equation,

$$\alpha_{A/B} (-) = (Y_A/Y_B)/(X_A/X_B) \tag{3}$$

where Y_A and Y_B represent mol fractions of components A and B in the permeable side, respectively. X_A and X_B represent mol fractions of components A and B in the feed side, respectively.

Membrane characterizations

A nano-permporometry test was performed using a Porometer Nano-6 (MicrotracBEL Corp.). Condensable vapor and inert gas were supplied to the membrane. The flow rate of inert gas in the permeable side was measured during the test. Because the pores in the membrane were filled by the condensation of vapor, the flow rate of inert gas decreased with increasing relative pressure of vapor. The relationship between the relative pressure of condensable vapor and the flow rate of inert gas represents the pore size distribution. Pretreatment was performed at 573 K for 3 h to remove adsorbed molecules on the membrane. In this study, Ar gas and n-hexane were used as the inert gas and condensable vapor, respectively. The measurement was taken at 333 K with the relative vapor pressure in the range of 0–0.3.

The micropore volume in the silicalite-1 membrane was evaluated by N_2 adsorption measurement. The measurement was performed non-destructively using BELSORP-max (MicrotracBEL Corp.). Pretreatment was performed at 573 K for 8 h under vacuum before the adsorption test. Adsorption measurements were carried out at 77 K.

Results and discussion

The n-hexane(n-Hex)/2,3-dimethylbutane(2,3-DMB) separation test was performed to investigate the effect of alkaline treatment on the permselectivity of the silicalite-1 membrane. The pore size

of silicalite-1 was approximately 0.55 nm, and the molecular diameters of n-Hex and 2,3-DMB were approximately 0.435 nm and 0.58 nm, respectively.[18] Therefore, if the silicalite-1 membrane had no defect, only n-Hex would penetrate through the micropores of the membrane because of the molecular sieving effect. In other words, the permeation of 2,3-DMB indicated the presence of defects that resulted in non-zeolitic pathways through the silicalite-1 membrane.

Fig. 1 shows the permeation and separation performance of a silicalite-1 membrane at 573 K as a function of the treatment period. When the alkaline treatment was carried out for 5 min, the 2,3-DMB permeance decreased from 4.52×10^{-10} to 1.29×10^{-10} mol m^{-2} s^{-1} Pa^{-1}, and the separation factor remarkably increased from 86.5 to 334. After further alkaline treatment for the total treatment period of 15 min, the 2,3-DMB permeance further decreased to 1.13×10^{-10} mol m^{-2} s^{-1} Pa^{-1}, resulting in the separation factor increasing up to 559.

The decrease in 2,3-DMB permeance by the alkaline treatment suggests the decrease of the non-zeolitic pathway through which 2,3-DMB is able to permeate. However, a slight increase in n-Hex permeance indicated that the micropores did not collapse after the alkaline treatment. Therefore, we considered that the non-zeolitic pathway in the silicalite-1 membrane was blocked by the alkaline treatment with CTAB while maintaining its micropores. In the following section, we discuss the reason why the membrane retained high permeation performance after the alkaline treatment.

When the alkaline treatment was performed up to 30 min, the 2,3-DMB permeance tended to increase. After a 70 min treatment, the 2,3-DMB permeance drastically increased to 2.38×10^{-8} mol m^{-2} s^{-1} Pa^{-1}, resulting in a decrease in the separation factor at 573 K to 3.13. The increase in 2,3-DMB permeance resulting from the longer periods of alkaline treatment would be caused by the creation of large non-zeolitic pathways through which 2,3-DMB penetrated by excess alkaline etching.

To confirm the reproducibility of this method, alkaline treatments were performed on four other silicalite-1 membranes using the same method. In all cases, 2,3-DMB permeances decreased and the separation factors increased in all membranes
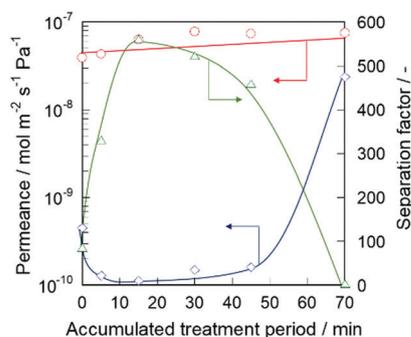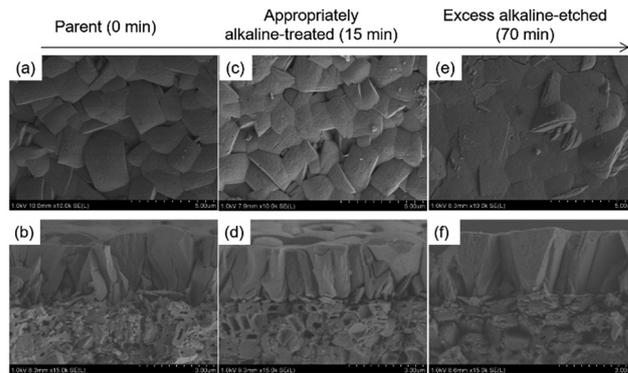

Fig. 2 FE-SEM images of alkaline-treated silicalite-1 membranes at each accumulated treatment period. (a), (c), and (e) membrane surfaces; (b), (d), and (f) cross-sections.

tested (as shown in Table ES1 in the ESI†), and we successfully affirmed the reproducibility. In addition, the treatment was carried out for other types of zeolite membranes (Na-*BEA, Na-ZSM-5, and Na-MOR), and then, the separation performances of these membranes increased as well (shown as Table ES2 in the ESI†).

Fig. 2 shows typical FE-SEM images of alkaline-treated silicalite-1 membranes during each treatment period. When the alkaline treatment was performed for 15 min, partial dissolution of seed crystals occurred, as shown in Fig. 2(d) (the dissolved part is represented by a blue arrow in the enlarged images shown in the ESI† as ES3). However, no significant change could be observed from the top view of the effective separation layer in the vicinity of the membrane surface, as shown in Fig. 2(c). After a 70 min treatment, crystals of the seed layer were severely collapsed by excess alkaline etching, and then large voids were visible among the seed crystals (Fig. 2(f)). In addition, the dissolution on the membrane surface was observed after the 70 min treatment, as shown in Fig. 2(e). The changes in the morphological features of the membrane after the 70 min treatment agreed with the results of the separation test.

A nano-permporometry test was performed to evaluate the changes in the non-zeolitic pathway during the alkaline treatment. Fig. 3 shows the ratio of the non-zeolitic pathway and separation factor of a treated silicalite-1 membrane. The ratio of the non-zeolitic pathway was obtained by dividing argon permeance at $p\,p_s^{-1}$ of 0.2 by the permeance at $p\,p_s^{-1}$ of 0 according to the method, which was proposed by Hedlund and his co-workers.[7,19]

When the alkaline treatment was performed for 5 min, the ratio of the non-zeolitic pathway decreased from 4.31×10^{-3} to 1.97×10^{-3}, and the separation factor increased from 86.5 to 332, as shown in Fig. 1. Furthermore, after the 15 min alkaline treatment, the ratio of the non-zeolitic pathway decreased and the separation factor increased as well. The non-zeolitic pathway in the silicalite-1 membrane was clearly healed in the early stage of alkaline treatment. When the alkaline treatment was prolonged up to 70 min, the ratio of the non-zeolitic pathway
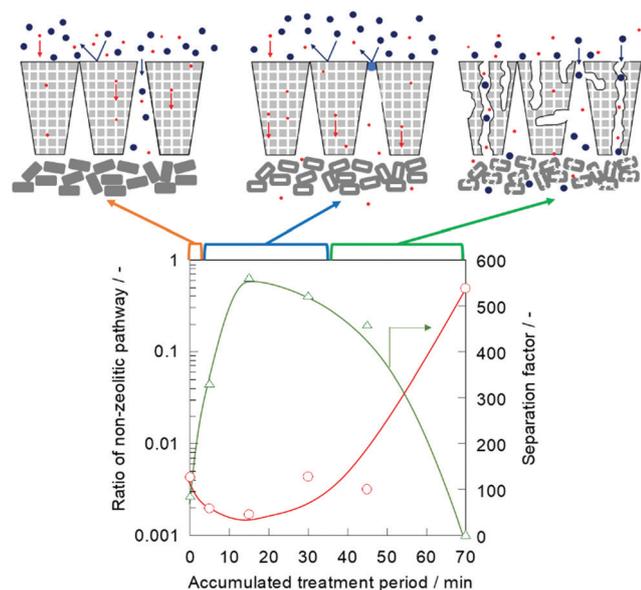

Fig. 1 Permeation and separation performance at 573 K of silicalite-1 membrane as a function of treatment period: ○, n-hexane; ◇, 2,3-dimethylbutane; △, separation factor.

Fig. 3 Relationship between the ratio of non-zeolitic pathway and separation factor (573 K).

remarkably increased to 4.91×10^{-1}, and the separation factor decreased to 3.13. This result indicated that the molecular sieving effect was obstructed because of the large number of non-zeolitic pathways formed by excess alkaline etching for a 70 min treatment.

The X-ray diffraction (XRD) measurement was performed to evaluate the changes in the crystallinity of the silicalite-1 membrane over the course of the alkaline treatment. Fig. 4 shows the XRD patterns of the silicalite-1 membrane during different treatment periods. No obvious reflection peaks other
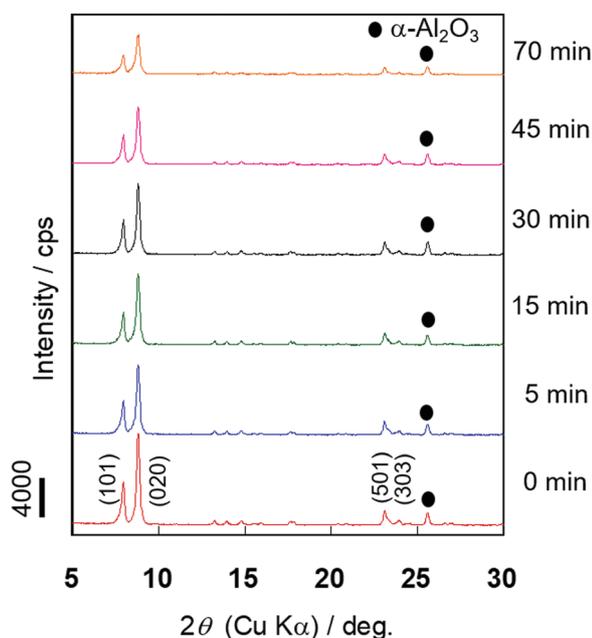

Fig. 4 XRD patterns of silicalite-1 membranes with different accumulated treatment periods.

than those corresponding to the MFI-type zeolite and support, α-alumina, were observed for all samples. There was little change in the intensities of the diffraction peaks assigned to the MFI-type zeolite until 30 min of alkaline treatment elapsed, suggesting that the crystal structure of MFI was maintained in the early stage of alkaline treatment. When the alkaline treatment was performed for >45 min, the intensities of the diffraction peaks decreased, suggesting that the crystal structure collapsed due to the progression of desilication.

Micropore volume, an index of crystallinity of zeolite, was evaluated by N_2 adsorption measurements to quantitatively determine the crystallinity change before and after the alkaline treatment. The volume of the micropores in the silicalite-1 membrane was obtained by the Saito–Foley (S–F) method.[20,21] The adsorption amount of N_2 at $p\,p_s^{-1}$ was 1.0×10^{-4}, and this number was adopted as the saturated adsorption amount in zeolite pores because this quantity represents the adsorbed amount required for the saturation of a cylindrical pore with a diameter of 0.55 nm, which is a size comparable to the MFI-type zeolite pore. In addition, we defined crystallinity as the ratio of micropore volume before and after the treatment.

Table 1 lists the accumulated treatment period and micropore volume. The micropore volume increased during the early stage of alkaline treatment for 15 min, and then, no significant change in micropore volume was observed after 45 min of prolonged alkaline treatment. The crystallinity decreased after the 70 min treatment, suggesting that the zeolite structure collapsed by excess alkaline etching.

The improvement in crystallinity by the alkaline treatment for zeolite powder has previously been reported in several studies.[12,22,23] These studies suggested that this phenomenon occurred because areas of poor crystallinity in zeolite were preferentially dissolved by the alkaline treatment, resulting in an overall higher crystallinity. We also considered that amorphous or low crystallinity parts in the silicalite-1 membrane were preferentially dissolved in the early stage of our alkaline treatment, and then, the micropore volume increased. The micropore volume should decrease after the treatment if alkalinity and surfactant remain in the micropore. This result also suggests that alkalinity and surfactant were successfully removed by washing and calcination after healing.

To study the roles of both NaOH and CTAB, treatments with only NaOH or CTAB aqueous solution were carried out, respectively. Table 2 lists the permeation and separation properties for each treatment.

Table 1 Accumulated treatment period and micropore volumes

Accumulated treatment period/min	Micropore volume/ 10^{-3} cm^3 g^{-1}	Crystallinity/%
0	9.20	100
15	9.84	107
30	9.97	108
45	9.86	107
70	8.62	94

Table 2 Separation and permeation properties of membranes with NaOH or CTAB

Membranes	Permeance/10^{-8} mol m^{-2} s^{-1} Pa^{-1}		Separation factor/—
	n-Hex	2,3-DMB	
M1 parent	4.84	0.235	20.6
M1 with NaOH	5.31	1.36	3.90
M2 parent	4.99	0.0687	72.6
M2 with CTAB	5.72	0.0721	79.3

The 2,3-DMB permeance of the silicalite-1 membrane treated with NaOH (aq) increased from 2.35×10^{-9} to 1.36×10^{-8} mol m^{-2} s^{-1} Pa^{-1}, and the separation factor decreased from 20.6 to 3.90 after only a 15 min treatment, indicating that without CTAB, NaOH treatment could easily result in the formation of a non-zeolitic pathway. In contrast, the permeation of 2,3-DMB into the silicalite-1 membrane treated with CTAB did not significantly change, and the separation factor also hardly changed. It was suggested that defects on the silicalite-1 membrane were not healed by CTAB molecules or cokes derived from CTAB calcination.

These results clearly showed that the combination of NaOH and CTAB was essential for the improvement of separation performance. CTAB has an important role as protector for the micropores of the silicalite-1 membrane during the alkaline treatment. We considered two hypotheses regarding the role of CTAB in our alkaline treatment. One of them is that CTAB protects micropores in a membrane by adsorbing on the external surface during alkaline treatment. Hui *et al.* reported that CTAB was adsorbed on the external surface of zeolite to protect the zeolite structure *via* multilayer adsorption during their alkaline treatment.[14] The other is that CTAB protects micropores by filling them. Iyoki *et al.* reported that treatment with a pore-filling hydroxide such as TEAOH and fluoride species resulted in *BEA-, MFI-, and MOR-type zeolite with high stability against high-temperature steaming by reducing the number of defect sites.[15] They noted that TEA cations worked as a pore filler to stabilize the framework during the treatment. Wang *et al.* reported that after alkaline treatment of ZSM-22, the templates were retained in the micropores.[24] The existence of retained templates in micropores increased the preservation of the zeolite crystal by hindering the contact between the desilication agent and Si–O–Si linkages.

We can conclude that the separation performance of the silicalite-1 membrane can be improved by this alkaline treatment possibly because non-zeolitic pathways between crystals are healed by amorphous silica leached from seed crystals and the low crystallinity parts. In other words, self-defect-healing occurred in the membrane by the use of a silica source derived from itself. Additionally, CTAB protects the micropores in a membrane while defect healing occurs.

Finally, we compared the effect of our alkaline treatment with other previously reported post-treatments for defect healing. Herein, the relative permeance and relative separation factor are defined as follows. The relative permeance is a ratio of permeance
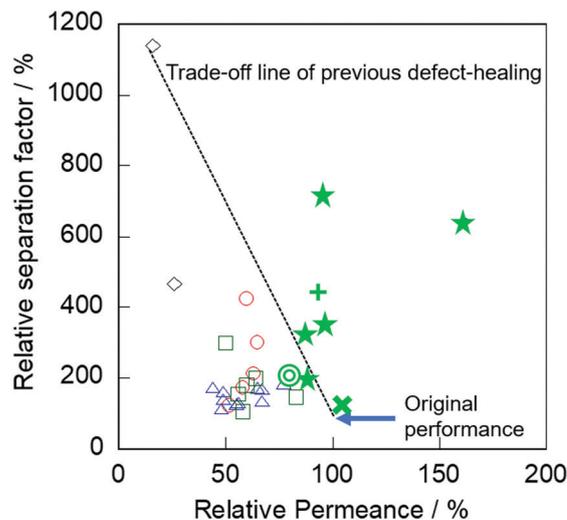

Fig. 5 Relative separation factor as a function of relative permeance in various treated membranes: ○, TEOS;[7,9] △, TEFS;[8] ◇, TIPB;[10] □, Dye;[11] ☆, AT with CTAB (this study) for silicalite-1; +, for Na-BEA membrane; ◎, for Na-MOR membrane; ×, for Na-ZSM-5 membranes.

obtained through the treated membrane and parent membrane: the relative separation factor is the ratio of the separation factor obtained through the parent and treated membranes as well. Fig. 5 shows the relative separation factor as a function of relative permeance in various treated membranes.

In previous post-treatments for defect healing,[7–11] significant degradation of permeation performance occurred by obstruction of micropores, as described in the Introduction. In contrast, our membranes exhibited no severe decrease in permeance by the alkaline treatment compared with the post-treatment methods previously reported. Specifically, the relative permeances after the alkaline treatment with surfactant were 88–160% with relative separation factors of 200–711%.

Conclusions

Separation performance was successfully increased by rapid alkaline treatment, and there was no decrease in permeability. The ratio of the non-zeolitic pathway in silicalite-1 membrane decreased, and the separation performance was improved by the use of both NaOH and CTAB. CTAB has an important role as a protector of micropores in the silicalite-1 membrane during alkaline treatment. The effectiveness of the treatment for other types of zeolite membranes (Na-*BEA, Na-ZSM-5, and Na-MOR) was also confirmed. This simple alkaline treatment with surfactant is a promising technique that can be used for defect healing of molecular sieving zeolite membranes.

Author contributions

M. Sakai designed the study and wrote the initial draft of the manuscript. H. Hori contributed to data collection and interpretation. All authors have approved the final version of the manuscript.

Conflicts of interest

There are no conflicts to declare.

Acknowledgements

References

1 D. S. Sholl and R. P. Lively, *Nature*, 2016, **532**, 435.

2 K. A. Thompson, R. Mathias, D. Kim, J. Kim, N. Rangnekar, J. R. Johnson, S. J. Hoy, I. Bechis, A. Tarzia, K. E. Jelfs, B. A. McCool, A. G. Livingston, R. P. Lively and M. G. Finn, *Science*, 2020, **369**, 310.

3 M. Y. Jeon, D. Kim, P. Kumar, P. S. Lee1, N. Rangnekar, P. Bai, M. Shete, B. Elyassi, H. S. Lee, K. Narasimharao, S. N. Basahel, S. Al-Thabaiti, W. Xu, H. J. Cho, E. O. Fetisov, R. Thyagarajan, R. F. DeJaco, W. Fan, K. A. Mkhoyan, J. I. Siepmann and M. Tsapatsis, *Nature*, 2017, **543**, 690.

4 P. Kumar, D. W. Kim, N. Rangnekar, H. Xu, E. O. Fetisov, S. Ghosh, H. Zhang, Q. Xiao, M. Shete, J. I. Siepmann, T. Dumitrica, B. McCool, M. Tsapatsis and K. A. Mkhoyan, *Nat. Mater.*, 2020, **19**, 443.

5 D. Kim, M. Y. Jeon, B. L. Stottrup and M. Tsapatsis, *Angew. Chem., Int. Ed.*, 2018, **57**, 480.

6 B. Min, S. Yang, A. Korde, Y. H. Kwon, C. W. Jones and S. Nair, *Angew. Chem., Int. Ed.*, 2019, **58**, 8201.

7 S. Karimi, D. Korelskiy, L. Yu, J. Mouzon, A. A. Khodadadi, Y. Mortazavi, M. Esmaeili and J. Hedlund, *J. Membr. Sci.*, 2015, **489**, 480.

8 N. Kosinov, V. G. P. Sripathi and E. J. M. Hensen, *Microporous Mesoporous Mater.*, 2014, **194**, 24.

9 M. Nomura, T. Yamaguchi and S. Nakao, *Ind. Eng. Chem. Res.*, 1997, **36**, 4217.

10 Y. Yan, M. E. Davis and G. R. Gavalas, *J. Membr. Sci.*, 1997, **123**, 95.

11 S. Hong, D. Kim, Y. Jeong, E. Kim, J. C. Jung, N. Choi, J. Nam, A. C. K. Yip and J. Choi, *Chem. Mater.*, 2018, **30**, 3346.

12 M. Ogura, S. Shinomiya, J. Tateno, Y. Nara, M. Nomura, E. Kikuchi and M. Matsukata, *Appl. Catal., A*, 2001, **219**, 33.

13 M. Ogura, S. Shinomiya, J. Tateno, Y. Nara, E. Kikuchi and M. Matsukata, *Chem. Lett.*, 2000, 882.

14 H. Liu, S. Xie, W. Xin, S. Liu and L. Xu, *Catal. Sci. Technol.*, 2016, **6**, 1328.

15 K. Iyoki, K. Kikumasa, T. Onishi, Y. Yonezawa, A. Chokkalingam, Y. Yanaba, T. Matsumoto, R. Osuga, S. P. Elangovan, J. N. Kondo, A. Endo, T. Okubo and T. Wakihara, *J. Am. Chem. Soc.*, 2020, **142**, 3931.

16 J. G. Martinez, M. Johnson, J. Valla, K. Lib and J. Y. Ying, *Catal. Sci. Technol.*, 2012, **2**, 987.

17 M. Sakai, T. Kaneko, Y. Sasaki, M. Sekigawa and M. Matsukata, *Crystals*, 2020, **10**, 949.

18 O. C. Gobin, S. J. Reitmeier, A. Jentys and J. A. Lercher, *J. Phys. Chem. C*, 2011, **115**, 1171.

19 D. Korelskiy, M. Grahn, J. Mouzon and J. Hedlund, *J. Membr. Sci.*, 2012, **417–418**, 183.

20 A. Saito and H. C. Foley, *AIChE J.*, 1991, **37**, 429.

21 A. Saito and H. C. Foley, *Microporous Mater.*, 1995, **3**, 531.

22 M. Bjørgen, F. Joensen, M. S. Holm, U. Olsbye, K. P. Lillerud and S. Svelle, *Appl. Catal., A*, 2008, **345**, 43.

23 A. Chawla, N. Linares, J. D. Rimer and J. G. Martínez, *Chem. Mater.*, 2019, **31**, 5005.

24 X. Wang, X. Zhang and Q. Wang, *Ind. Eng. Chem. Res.*, 2019, **58**, 8495.